

Stationary Pattern of Vortices or Strings in Biological Systems: Lattice Version of the Lotka-Volterra Model

Kei-ichi Tainaka

Department of Physics, Ibaraki University, Mito 310, Japan

(Received 1 August 1989)

By stochastic simulation, we investigate the spatial pattern in the biological system composed of three competing species. Topological defects are introduced to explain the pattern formation in this system. The spatial dimension d determines the nature of defects such as kinks, vortices, and strings. When $d=2,3$, the system approaches the stationary state, where the peculiar defect configuration is found.

PACS numbers: 87.10.+e, 64.60.Cn

Ecological studies heretofore have been mainly aimed at the spatial and temporal evolution of the number (density) of individuals. In this Letter, we introduce the concept of topological defects. The importance of topological defects is widely recognized in many different areas.¹ Since the number of topological defects is much less than that of individuals, the pattern process of the system is very simplified.

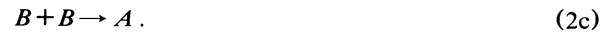
Many authors have considered the population dynamics concerning the struggle for existence. A typical example is the Lotka-Volterra model.² We can regard this model as the gas system composed of three competing species (1, 2, and 3). By the collision (reaction), the particles (individuals) change their species. When a pair of particles of species i and j ($i \geq j$ and $i, j=1,2,3$) react, they change into two particles of species i , if $i-j=0,1$. If $i-j=2$, they change into two particles of species j . Thus, the relation of "strength" between the species is cyclic. The number (density) of each species in this gas system is given by

$$\dot{n}_i \propto n_i(n_{i-1} - n_{i+1}), \quad (1)$$

where the dot represents the derivative with respect to time, and $n_{i+3}=n_i$. Equation (1) is called the Lotka-Volterra model whose solution gives the oscillation profile of $n_i(t)$ depending on the initial condition.³

Recently, the present author applied the Lotka-Volterra model to a lattice system.⁴ In this system each lattice site is occupied by one particle of three species, and the collision of a particle is limited to take place with the neighboring one. The simulation was performed by asynchronous processing (random collision). The dynamics of the lattice Lotka-Volterra (LLV) system is entirely different from the result of (1). The lattice dimension d strongly influences the dynamics. When $d=1$, the number n of "domains" (regions occupied by particles of the same species) decreases with time as $n \propto t^{-\alpha}$. We have obtained $\alpha \sim 0.8$ for the initial condition $n_1:n_2:n_3=1:1:1$, and $\alpha \sim 1.2$ for 7:2:1. When $d=2$, the system approaches the stationary state regardless of initial conditions. The pattern of domains in the stationary state varies greatly with time.

In this Letter, we introduce topological defects to explain the pattern formation in the LLV system. The system is subdivided into many domains. The particle in each domain never changes its species, unless it locates at the boundary. For $d=1$ we regard the domain boundary as a defect. This concept of the defect is similar to the "kink" in the one-dimensional (1D) Ising model.^{5,6} There are two types (A and B) for the defect. When particles are lined up on the abscissa, the domain boundaries move to the right (defect A) or left (defect B). These defects react as



The number of particles A is generally unequal to that of B .

It is natural first to examine the dynamics of the LLV system in the mean-field approximation (MFA). For (2), MFA leads to

$$\begin{aligned} \dot{a} &= -k(ab + a^2 - b^2), \\ \dot{b} &= -k(ab + b^2 - a^2), \end{aligned} \quad (3)$$

where a and b are the density of defects A and B , respectively, and k is a constant (we assume $k=1$). By putting $s=a-b$ and $n=a+b$, we get $(3n^2+s^2)^2=Cs$, where C is a constant. This solution indicates that s rapidly vanishes and then n decreases with time as $n \propto t^{-\alpha}$ ($\alpha=1$). Thus, MFA gives a fairly good result concerning the value of α . However, further simulation shows the following different results compared to those predicted from MFA: (1) The density b (or a) rapidly decreases compared to a (b) from the early-time stage ($t > 10$), where the time t is measured by the unit of Monte Carlo (MC) step. (2) In the latter stage ($a \gg b$) we find $\alpha \sim 0.5$. This can be accounted for as follows; for $a \gg b$, reaction (2b) becomes relevant. Since (2b) takes place in the diffusion-controlled limits, we obtain $n \sim a \propto t^{-0.5}$.^{7,8}

When $d=2$, the topological defect is represented by

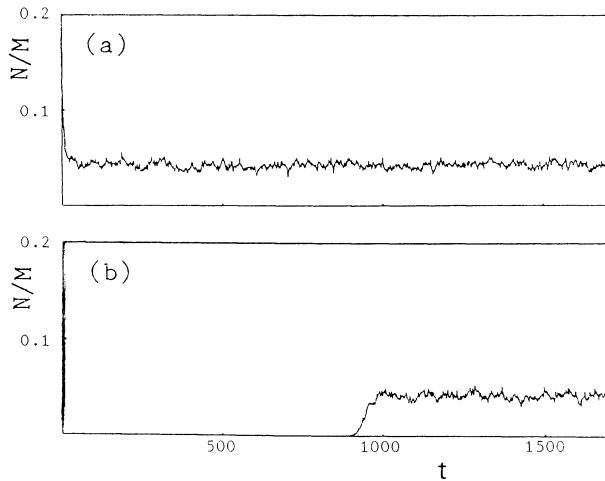


FIG. 1. Time evolution of the number N of vortices for the square lattice ($M=200 \times 200$). At $t=0$, the species are distributed (a) randomly, and (b) as a tricolor flag.

the “vortex” defined by the point of contact between three different domains. Three domains rotate around the vortex. There are two kinds of vortices (V_R and V_L) distinguished by the direction of the rotation. These vortices move in a complicated manner as a particle, and are never annihilated or created except for the following reaction:



Under the periodical boundary condition, the numbers of V_R and V_L are always equal to each other (conservation law). The properties of the vortices are similar to those in the 2D superfluid.⁹ However, the rotation speed (v) around the center of the vortex is different. In the case of our vortex, $v(r)$ at the distance r from the center does not depend on r , although $v \propto r^{-1}$ for the vortex in (super)fluid. We performed the simulation of random collision and obtained the total number of vortices $N(t)$ for different initial conditions; see Fig. 1, where M is the total number of lattice sites. It is found from Fig. 1(b) that it takes a long time to reach the stationary state for the initial condition $N(0)=0$. This result suggests that the creation rate of vortices depends upon the density of vortices present. In Fig. 2, the number of vortices which are created or annihilated during one MC period from $t - \frac{1}{2}$ to $t + \frac{1}{2}$ are plotted. It is found from Fig. 2 that the average creation rate is proportional to the total vortex number N . This result is similar to photon creation in stimulated emission. We can further confirm, from a video visualizing the defect dynamics, that the vortices are not equally created at every site (unequal creation). The creation rate decreases in a region where the density of vortex is low.

Snapshots of the vortex pattern are displayed in Fig. 3, where (a) and (b) represent the initial and stationary

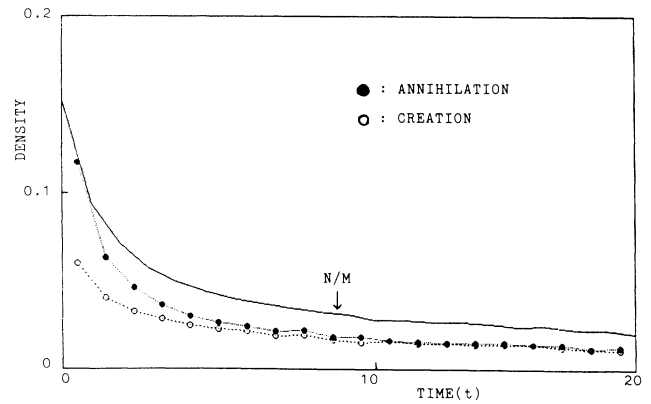


FIG. 2. Average rates of creation and annihilation of vortices per MC step. At $t=0$, species are randomly distributed ($M=150 \times 150$).

states, respectively. Although the defect pattern in the stationary state greatly varies with time, it has invariant features: First, there are large voids where the vortex is empty. Second, vortices locate with negative correlation; i.e., located around a vortex of type V_R are the other type of vortices. The appearance of voids in the stationary configuration is also explained by the unequal creation.

When $d=3$, the dynamics is characterized by the “vortex line (string),” which is a sequence of vortices. Every string closes, under the periodical boundary condition. Since the species rotate around the string (loop), each string has its own direction of rotation. The loop grows or shrinks, and sometimes gives rise to reconnection. Thus, our strings resemble the vortex lines in superfluid¹⁰ or the cosmic strings.^{11,12} The string in our model has several properties that are different from other strings: (1) Strings can be created inside the system; (2) our string is discrete. By the latter feature, we can easily find the elementary process of the string dynamics.

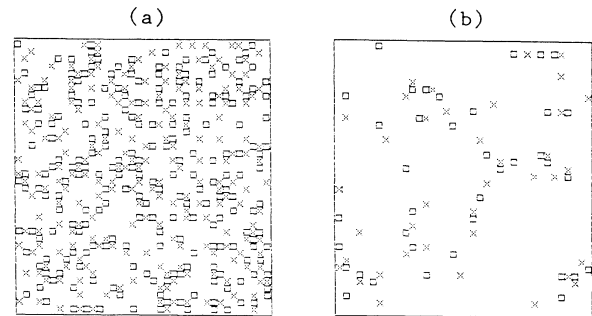


FIG. 3. Snapshot of vortex pattern for the square lattice ($M=38 \times 38$); \times denotes V_R , \square denotes V_L : (a) initial state, where the species are randomly distributed; (b) stationary state ($t=200$).

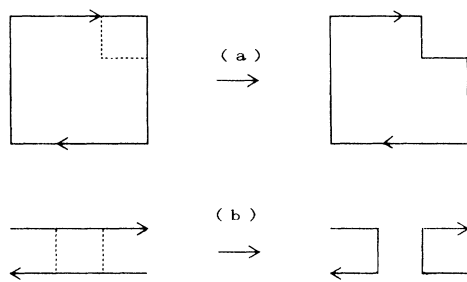


FIG. 4. Examples of the elementary process representing the shape change of strings: (a) shrinkage; (b) reconnection. The solid lines denote the string defects, and the arrows on the strings indicate the direction of the rotation of the species. In both processes, the unit strings disappear.

Whenever the loop changes its shape, the unit ring (U_R) of defect is annihilated or created for one collision step:

$$U_R \rightleftharpoons \phi. \quad (5)$$

Here, U_R is the smallest unit ring. For the cubic lattice, U_R denotes the square loop with a side of the lattice size. Two examples for the annihilation process of U_R are illustrated in Fig. 4, where (a) and (b) represent the shrinkage and reconnection of strings, respectively. In both steps, the unit rings with clockwise direction vanish. Note that each dotted line (no defect) in Fig. 4 must be regarded as the sum of two line defects which have inverse directions to each other.

The dynamics for the 3D-LLV system reveals that the total length of strings (L) approaches a unique value (stationary state), as in Fig. 1 for $d=2$. The process leading to the stationary state is very complicated depending on initial conditions. An example is illustrated in Fig. 5, where (a) represents the distribution of species at $t=0$ (the string is therefore absent). The configurations of strings are visible in Figs. 5(b), 5(c), and 5(d). In the early-time stage ($t = \frac{1}{4}$) several loops (rings) are created. The axes of the rings point in the same direction, since the creation of the rings is attributed to the fact that the species 3 in Fig. 5(a) contacts with 1 penetrating 2. The snapshot in the steady state [Fig. 5(d)] illustrates several features: (i) Large voids are found as for $d=2$; (ii) the shape of the large strings is complicatedly entangled. These are invariant features irrespective of initial distributions. This entanglement in the stationary state may be explained by the unequal creation. In the region where string density is high, many unit rings are frequently created or annihilated. In this situation, the string forms a complicated configuration.

In summary, pattern formation in the LLV system is simplified by defect reactions. For $d=1$ (2) it is revealed that the total number of defects monotonically decreases, and at the final stage all defects vanish. On the

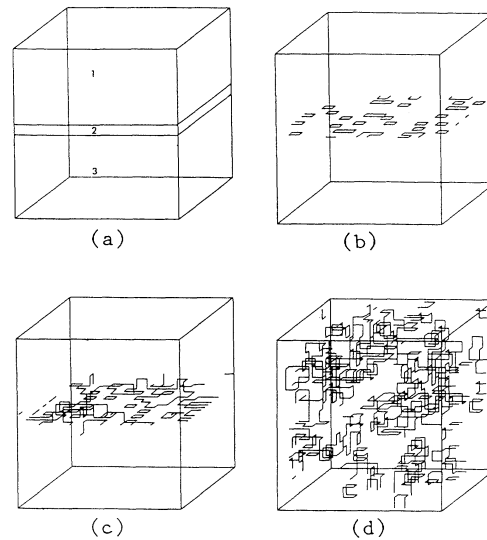


FIG. 5. The case study of the pattern formation of strings ($16 \times 16 \times 16$ cubic lattice); (a) initial distribution of three species. String configuration at (b) $t = \frac{1}{4}$, (c) $t = 1$, and (d) $t = 100$ (stationary state).

other hand, reaction (4) or (5) predicts the existence of a stationary state, when the creation and annihilation of the defects are equally balanced. The vortex number N_s and the total length of strings L_s in the stationary state becomes

$$N_s/M \sim 0.04, \quad L_s/M \sim 0.06. \quad (6)$$

Stationary states can be easily confirmed by obtaining the number of the topological defects (see Fig. 1).

In the string system, we presented (5) as the elementary process of the dynamics. It is natural to conclude from (5) that for the order parameter the number of unit rings (N_U) to construct whole strings is more appropriate than the total length of strings (L). For example, the value of L is unchanged for the process in Fig. 4(a), although N_U decreases from nine to eight unit rings. We can easily confirm that Fig. 4(a) is the process leading to the ordered state. The value of N_U means "area" for the loop, while L represents the "perimeter" in this figure. Unfortunately, however, it is difficult to obtain N_U for the actual system.

The defect densities (6) in the stationary state can be altered by a slight modification of our model. For $d=2,3$, a phase transition similar to the Kosterlitz-Thouless type may be found. In this case, the transition parameter (temperature in the usual physical systems) had a biological meaning. Various types of defect dynamic in the LLV system will be simulated with short computational time.

The author is indebted to Professor Y. Itoh for his valuable advice and to J. Kimura and N. Tsuji for help with the computer simulation.

¹*Physics of Defects*, edited by R. Balian, M. Kleman, and J.-P. Poirier (North-Holland, Amsterdam, 1981).

²*Synergetics, an Introduction*, edited by H. Haken (Springer-Verlag, Berlin, 1977), p. 130.

³Y. Itoh, *Ann. Inst. Statist. Math.* **25**, 653 (1973); *Prog. Theor. Phys.* **78**, 507 (1987).

⁴K. Tainaka, *J. Phys. Soc. Jpn.* **57**, 2588 (1988).

⁵G. F. Mazenko and P. S. Sahni, *Phys. Rev. B* **18**, 6139 (1978).

⁶K. Kawasaki and T. Ohta, *Physica (Amsterdam)* **116A**, 573 (1982).

⁷D. Toussaint and F. Wilzeck, *J. Chem. Phys.* **78**, 2642 (1982).

⁸S. Kanno and K. Tainaka, *Prog. Theor. Phys.* **80**, 999 (1988).

⁹E. Webster, G. Webster, and M. Chester, *Phys. Rev. Lett.* **42**, 243 (1979).

¹⁰K. W. Schwarz, *Phys. Rev. Lett.* **49**, 283 (1982); *Phys. Rev. B* **31**, 5782 (1985).

¹¹D. P. Bennett and F. R. Bouchet, *Phys. Rev. Lett.* **60**, 257 (1988).

¹²A. Albrecht and N. Turok, *Phys. Rev. D* **40**, 973 (1989).